EUROPEAN ORGANIZATION FOR NUCLEAR RESEARCH

DIRAC Collaboration status report to SPSC, October 2021

L. Nemenov (JINR), on behalf of the DIRAC Collaboration

1. K^+K^- pair analysis in the effective mass region near $2m_K$

DIRAC experiment investigated in the reaction p(24 GeV/c) + Ni the particle pairs K^+K^-, $\pi^+\pi^-$ and pp^- with relative momentum Q in the pair center mass system (c.m.s.) less than 100 MeV/c. Because of background studies, DIRAC explored three subsamples of K^+K^- pairs, obtained by subtracting – using time-of-flight (TOF) technique – background from initial Q distributions with K^+K^- populations more than 70%, 50% and 30%. In the two runs with the data sets DATA2 and DATA3, DIRAC identified about 11000 K^+K^- pairs (30% subsample). Half of these pairs lie in the effective mass interval $2m_K$ to $2m_K + 0.8$ MeV.

The corresponding pair distributions in Q and in its longitudinal projection Q_L were analyzed first in a Coulomb model, which takes into account only Coulomb final state interaction (FSI) and assuming point-like pair production. In order to study contributions from strong interaction, a second more sophisticated model was applied, considering besides Coulomb FSI also strong FSI via the resonances $f_0(980)$ and $a_0(980)$ and a variable distance $r*$ between the produced K mesons. This analysis was based on the three theoretical models: Achasov, Martin and ALICE collaboration. These models used the different parameter sets for the pairs production description.
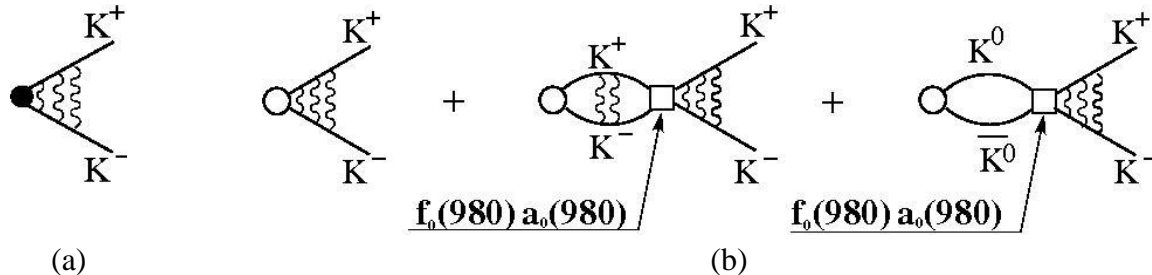

(a)   (b)

Fig. 1: The schematic description of K^+K^- production processes. a) The black point presents the pair point-like production; the wavy lines describe the Coulomb interaction in the final state. b) The circle and square present the pair non point-like production and strong interaction in the final state respectively.

1.1 Coulomb analysis

In the Coulomb analysis the K^+K^- pairs numbers were evaluated from the experimental Q_L and Q distributions which have different shapes.

On Fig.2 is shown the Q_L spectrum of 70%, 50% and 30% subsamples for the DATA3/DATA2. Each subsample was obtained by subtraction of the background from the experimental distributions with 70%, 50% and 30% of the K^+K^- pairs. Simulated distributions of K^+K^- pairs (Coulomb parametrization) and residual background of $\pi^+\pi^-$ and $p\bar{p}$ pairs are fitted the experimental spectrum in the interval $0 < Q_L < 100$ MeV/c. The red line is the K^+K^- distribution, the black line is the sum of K^+K^- and residual background. In the subsamples 70% and 30% the residual background is small and the lines coincide practically. For K^+K^- pairs in the region of Q_L smaller than 10MeV/c the Coulomb enhancement is clearly visible whereas the residual background is small and practically uniform.
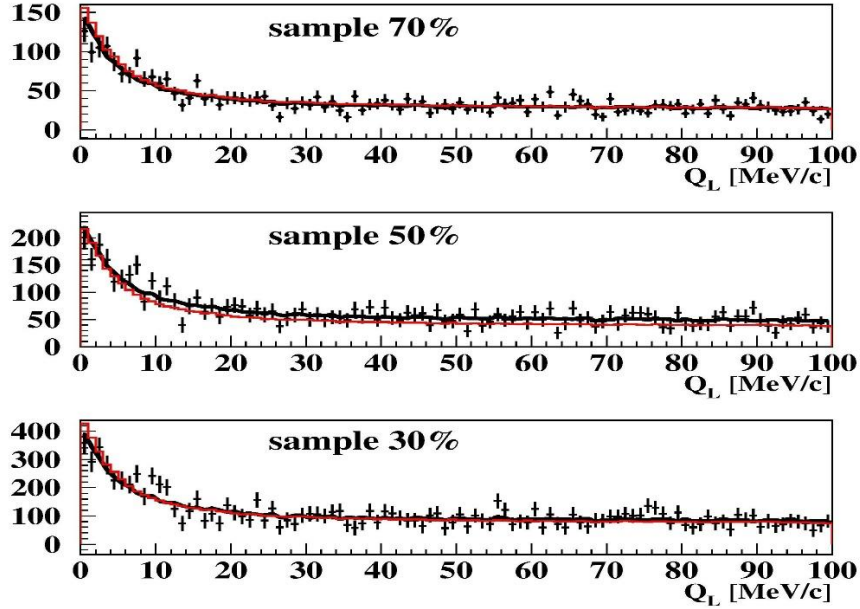

Fig. 2: Q_L distributions of the subsamples 30%, 50% and 70% for DATA3/ DATA2. The experimental spectra in the interval $0 < Q_L < 100$ MeV/c are fitted by simulated K^+K^- (point-like, Coulomb FSI) and residual $\pi^+\pi^-$ and p-anti-p background distributions. The red curve is the K^+K^- distribution, the black one is the sum of K^+K^- and residual background distributions. In the subsamples 70% and 30% the residual background is small and these curves practically coincide. For K^+K^- pairs in the region of $Q_L < 10$ MeV/c the Coulomb enhancement is clearly visible, whereas the residual background is small and practically uniform.

Table 1: Matching pair numbers for Q and Q_L distribution analyses. The errors of K^+K^- and background values are the same.

	cut on ToF	distribution	K^+K^-	$\pi^+\pi^-$ & $p\bar{p}$ background
DATA2 + DATA3	70%	Q	3900 ± 410	-110
		Q_L	3930 ± 580	-140
	50%	Q	5320 ± 730	1100
		Q_L	5460 ± 1020	960
	30%	Q	11220 ± 1370	180
		Q_L	10750 ± 2020	300

It is seen from Table 1 that the K^+K^- pairs number defined on Q and Q_L distributions do not differ significantly.

1.2 Data analysis assuming non point-like K^+K^- pair production and Coulomb and strong K^+K^- interaction in the final state

The distributions in r^*, the distance between K^+ and K^- in their c.m.s. connecting with the K mesons from the decay of short-lived sources and long-lived resonances is described as the sum:

$$w_g * Gauss + w_{K^*} * K^*(892) + w_\Lambda * \Lambda(1520) + w_\varphi * \varphi(1020).$$

The first term describes the contributions of the short-lived sources approximated by Gaussian with the radius $r_0 \approx 1.5\,fm$, the other terms describe the contributions of the three resonances. The w_i are the relative contributions of the different sources in K^+K^- pairs production; the sum of w_i is equal to unity. The weight values and their errors were evaluated. The analysis was performed for the three sets of w_i.

The first extreme set (0.00, 0.76, 0.10, 0.14) maximizes contributions of the K(892), Λ(1520) and φ(1020) resonances producing the largest value of the average r^* ; the third extreme set (0.57, 0.35, 0.06, 0.02) maximises the role of the short-lived K^+K^- pair sources generating the minimum value of the average r^* and the second set (0.10, 0.76, 0.08, 0.06) uses the intermediate values of w_i.

The distributions in Q (fitting curves) were calculated for each of DATA2 and DATA3 and for each subsample using three theoretical parametrizations of Achasov, Martin and ALICE. The experimental data of the 70% subsample were analysed by a dedicated fitting curve with $\pi^+\pi^-$ and pp^- background. The results are shown in the Table 2.

The difference between extreme yield values gives the maximum numbers of systematic errors in connection with the uncertainty of r* distribution. The maximum errors values are ±70, ±55 and ±40. These systematic errors are significantly smaller than the errors in Table 2. Therefore for the analysis of the two other experimental subsamples only the intermediate distribution on r^* was used.

The results of 70%, 50% and 30% subsamples are presented in the Table 2. It is seen that for any subsample the Achasov approach gives the residual background deflection from zero significantly larger than Martin and ALICE calculations. The large level of residual background can be considered as the result of insufficient accuracy of the fitting curve describing of K^+K^- distribution in Q.

Table 2: Pair numbers in the DATA3/ DATA2. The number of K^+K^- and background pairs (in brackets) were evaluated by fitting experimental distributions in Q in three subsamples by K^+K^- distributions, calculated with different parametrizations. The errors of K^+K^- and background pairs are identical.

	Achasov K^+K^- (backgr.)	Martin K^+K^- (backgr.)	ALICE K^+K^- (backgr.)	Total events
70% sample				3790
maximum r^*	3190 ± 330	3650 ± 370	3720 ± 380	
intermediate r^*	3120 ± 320 (670)	3600 ± 360 (190)	3680 ± 370 (110)	
χ^2/ndf DATA3/DATA2	1.03/1.20	1.00/1.18	1.00/1.18	
minimum r^*	3050 ± 320	3540 ± 360	3640 ± 370	
50% sample				6420
intermediate r^*	4340 ± 570 (2080)	4940 ± 640 (1480)	5040 ± 660 (1380)	
χ^2/ndf DATA3/DATA2	0.80/1.04	0.79/1.04	0.78/1.05	
30% sample				11030
intermediate r^*	9230 ± 1080 (1800)	10500 ± 1220 (530)	10680 ± 1240 (350)	
χ^2/ndf DATA3/DATA2	0.70/0.89	0.68/0.88	0.68/0.88	

Therefore the experimental data will be analysed in ALICE and Martin approximation only. The large residual background in the 50% subsample indicates that this experimental distribution is less reliable than in the two other subsamples.

The Figure 3 shows the experimental distributions in Q, fitting curves describing K^+K^- pairs (ALICE approach), and sum of fitting curves and residual backgrounds.

It is seen that for 70% (30%) subsample the fitting curve alone describes well the experimental distribution in the total interval of Q demonstrating that admixture of the residual background to the K^+K^- pairs is relatively small. This result is in agreement with the average level of the residual background, which is equal to 3% (3.2%) of the total number of events in the distribution.

The same analysis was done for the 50% subsample in which the residual background level is larger than that in the two other subsamples.

The corrected experimental distributions (ALICE parametrization) were obtained after background subtraction and is shown in Fig. 4. The red and the blue fitting curves on the Fig. 4 were evaluated from the analysis of experimental distributions with residual background in Coulomb and Martin parametrization respectively.

It is seen that Martin and Coulombs fitting curves describe the corrected experimental distributions well. The small difference between Martin and Coulomb parametrization in the interval 30-100MeV/c caused by strong K^+K^- interaction in the final state which is taken into account only in Martin approach.
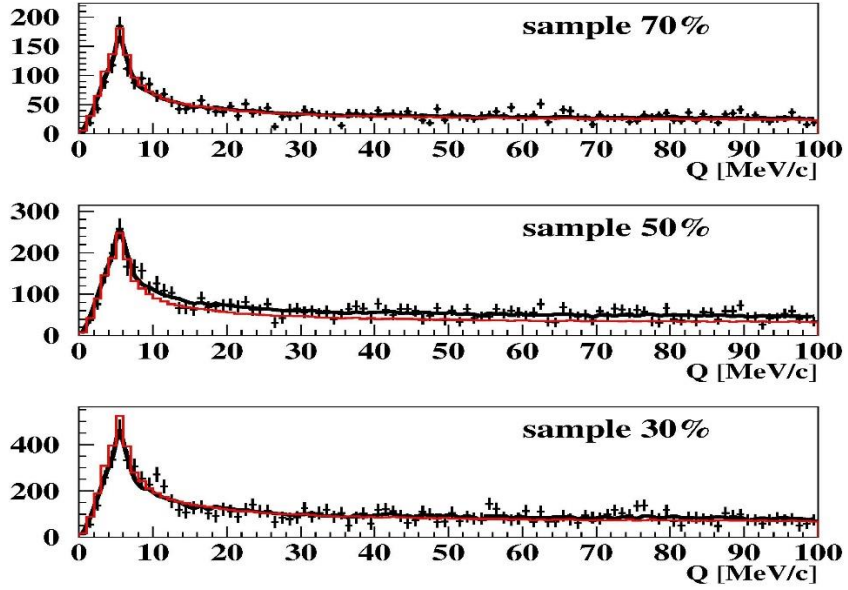
4

Fig. 3: Q distributions of the subsamples 30%, 50% and 70% for DATA2 and DATA3. Simulated distributions of K^+K^- (ALICE parametrization) and residual background of $\pi^+\pi^-$, accidental and p-anti-p pairs are fitting the experimental spectrum in the interval $0 < Q < 100$ MeV/c. The red line is the K^+K^- distribution, the black line is the sum of K^+K^- and residual background. In the subsamples 70% and 30% the residual background is small and these lines practically coincide.
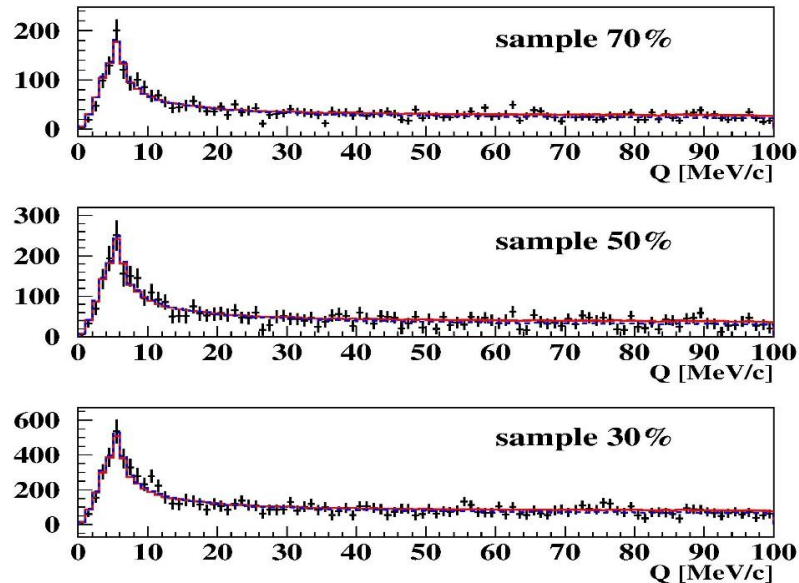

Fig. 4: Q distributions in the interval 0-100 MeV/c of K^+K^- (ALICE parametrization) of the subsamples 30%, 50% and 70% for the DATA3/ DATA2 after residual background subtraction. The red and the blue fitting curves were evaluated from the analysis of experimental distributions with residual background in Coulomb and Martin parametrizations respectively. It is seen that the difference between these curves is not significant and they describe "pure" experimental K^+K^- distributions well.

5

The distributions in the interval 0-30MeV/c are presented in Fig. 5.

It is seen that the Martin and Coulomb fitting curves, presented as histograms, are in this region coinciding and describing well the corrected experimental data.

The efficiencies of all cuts are known. Using these efficiencies, the total numbers of detected K^+K^- pairs in 70%, 50% and 30% subsamples were evaluated. They are 40890±4110, 29650±3880 and 38140±4430 pairs respectively.
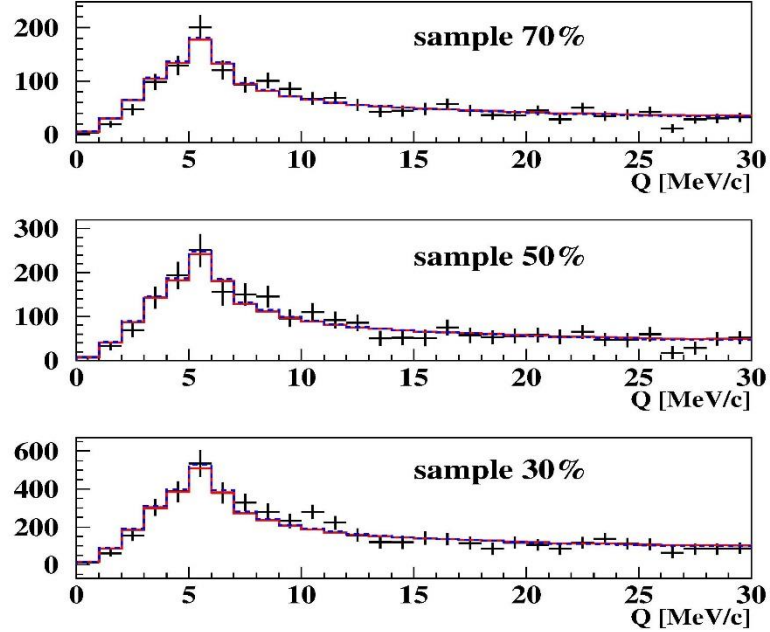

Fig. 5: Q distributions in the interval 0-30 MeV/c of K^+K^- (ALICE parametrization) of the subsamples 30%, 50% and 70% for the DATA3/ DATA2 after residual background subtraction. The red and the blue fitting histograms were evaluated from the analysis of experimental distributions with residual background in Coulomb and Martin parametrizations respectively. It is seen that in this interval of Q the difference between these histograms is absent and they describe "pure" experimental K^+K^- distributions well.

The background in the 30% subsample is about 19 times larger than in the 70% subsample. Nevertheless the total numbers of K^+K^- pairs are in good agreement demonstrating that the background and residual background subtraction was done correctly. The K^+K^- pairs number in the 50% subsample differs from two others values by 2 standard errors, confirming as mentioned above that experimental data in this subsample is less reliable. The total number of K^+K^- pairs calculated using Martin approach differs from the obtained numbers significantly less than the presented errors.

2. Proton-antiproton pairs analysis

The shape of detected proton-antiproton pairs in the relative momentum Q is expected to be more sensitive to the size of the particle production region compared to the case of detected K^+K^- pairs. Thus, the study of this shape could open a possibility to evaluate the size of pairs production region. The preliminary results of the $p\bar{p}$ pairs distribution in Q_L were evaluated by subtraction of the similar spectra of K^+K^- and $\pi^+\pi^-$ pairs from the experimental distribution of all pairs. The relative number of $p\bar{p}$ pairs in the experimental distribution before the background subtraction was 50%. The $p\bar{p}$ pairs distribution in Q_L is presented on Fig.6 by black points. The blue histogram shows the K^+K^- pairs simulated spectrum calculated in the Coulomb parametrization and fitting experimental K^+K^- pairs distribution. This histogram fits the $p\bar{p}$ pairs distribution in Q_L interval 50MeV/c-100MeV/c. It is seen that for low Q_L values the Coulomb FSI enlarges the $p\bar{p}$ pairs yield significantly more than K^+K^- pairs. The pairs yield dependence in Q_L is proportional to the value of Coulomb correlation function Ac(Q_L). Its value is around unity at large Q and is increasing when Q decreases. For small Q the Coulomb correlation function is proportional to $1/v$, where v is the relative velocity in the pair c.m.s. For the same Q value the relative velocity in $p\bar{p}$ pair is a factor two less than v in K^+K^- system. Therefore the yield of $p\bar{p}$ pairs at small Q_L is significantly larger than the K^+K^- pairs yield.

The investigation of proton-antiproton system in the region of relative momentum from zero to 100MeV/c will be finished in 2022.
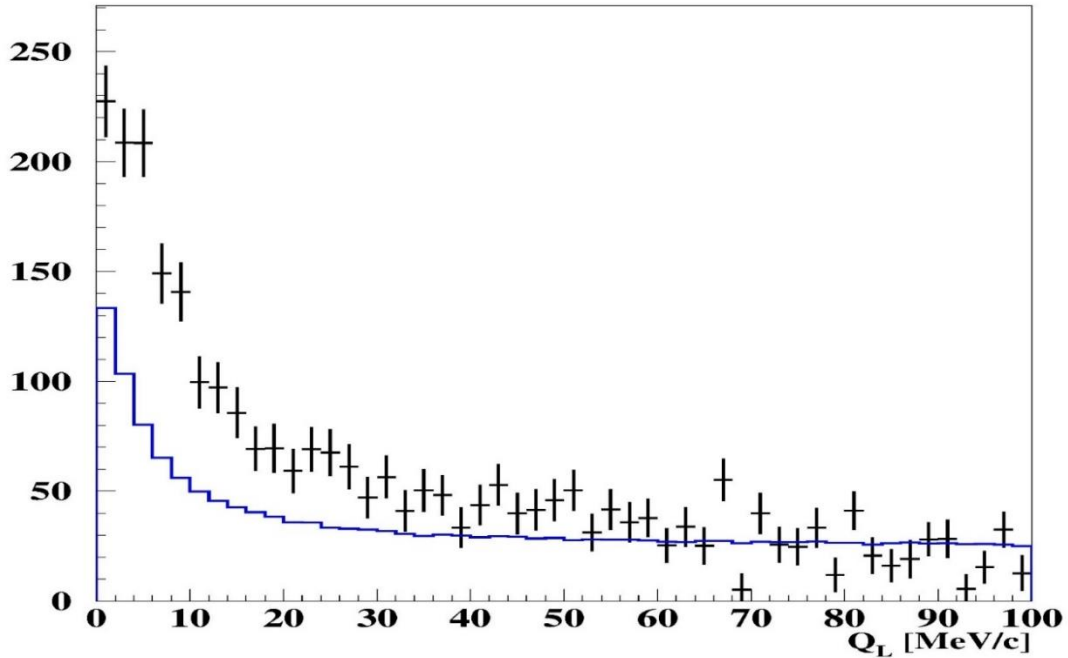

Fig. 6: Q_L distribution of $p\bar{p}$ pairs (black points). The blue histogram shows the K^+K^- pairs simulated spectrum calculated in the Coulomb parametrization and fitting experimental K^+K^- pairs distribution. This histogram fits the $p\bar{p}$ pairs distribution in Q_L interval 50MeV/c-100MeV/c. It is seen that for low Q_L values the Coulomb final state interaction enlarges the $p\bar{p}$ pairs yield significantly more than K^+K^- pairs.

3. The first evaluation of the K⁺K⁻ atoms number.

The K⁺K⁻ pairs analysis at $Q_L <$ 30MeV/c shows that Coulomb parametrization describes at small Q_L the experimental data well: the difference between distributions calculated in Martin and Coulomb parametrizations is significantly less than experimental errors (see Fig.5), demonstrating that at small Q the main contribution to the FSI gives the Coulomb interaction.

In this case (see Fig.1a) there is the relation between the number of K+K- pairs with the small Q_L and the number of K⁺K⁻ atoms generated in the experiment. It allows by model independent way to calculate in the first time the number of produced K⁺K⁻ atoms and to formulate the conditions of this atoms observation and their lifetime measurement.

This work will begin in 2022.

4. The short-lived π⁺π⁻ atom lifetime measurement

Previously, the π⁺π⁻ pairs obtained in DATA3/DATA2 were used only as a calibration process for the πK and K⁺K⁻ pairs analysis. We expected better statistics of the π⁺π⁻ pairs compared to our previously published result. The preliminary results on the measurement of short-lived atom lifetime and π⁺π⁻ scattering length based on these data will be presented in 2023.